

6 High Relaxivity Contrast Agents for MRI and Molecular Imaging

S. Aime, A. Barge, E. Gianolio, R. Pagliarin, L. Silengo, L. Tei

6.1	Introduction	99
6.2	Determinants of Relaxivity	103
6.3	How to Improve Relaxivity	105
6.3.1	Interactions of Gd(III) Complexes with Proteins	105
6.3.2	Effect of the Water Exchange Rate on Relaxivity	107
6.4	Targeting Cells with Gd(III) Chelates	111
6.5	Concluding Remarks	118
	References	119

6.1 Introduction

The superb spatial resolution and the outstanding capacity of differentiating soft tissues have determined the widespread success of magnetic resonance imaging (MRI) in clinical diagnosis (Young 2000; Rinck 2003). The main determinants of the contrast in an MR image are the proton relaxation times T_1 and T_2 . When there is a poor contrast between healthy and pathological regions due to a too-small variation in relaxation times, the use of a contrast agent can be highly beneficial. Contrast agents are chemicals able to alter markedly the relaxation times of water protons in the tissues where they distribute. Their use has led to remarkable improvements in medical diagnosis in terms of higher specificity, better tissue characterization, reduction of image artifacts, and functional information. Depending on whether the dominant effect occurs mainly on T_1 or

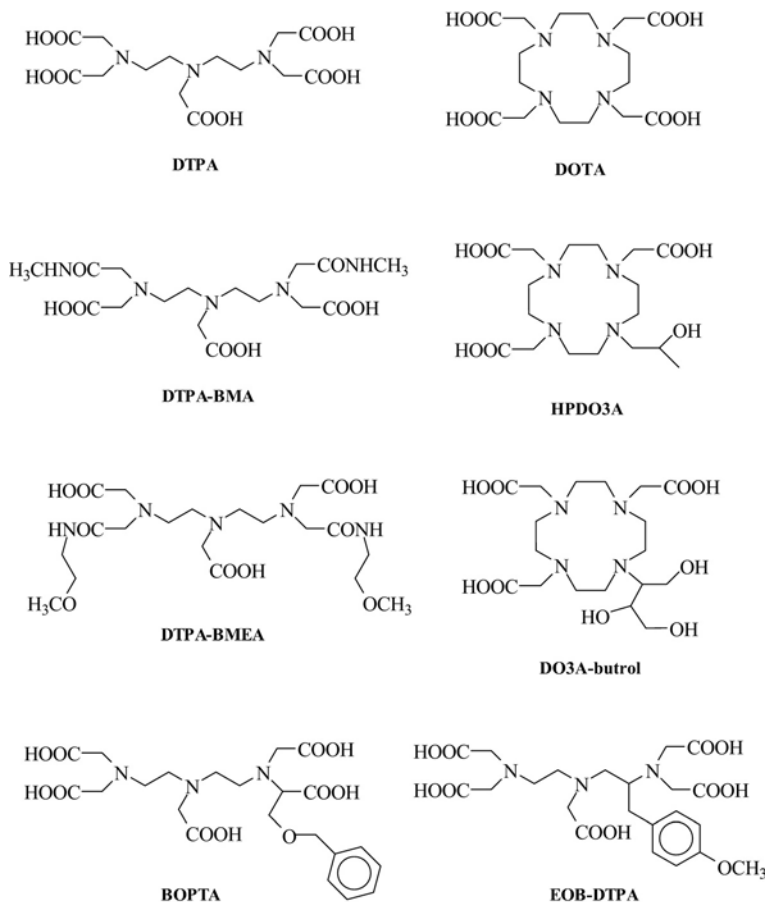
T_2 , MRI contrast agents can be classified as positive or negative agents, respectively. The most representative class of T_1 -positive agents is represented by paramagnetic Gd(III) chelates, whereas iron-oxide particles represent the class of T_2 -negative agents (Merbach and Toth 2001).

Currently, about one-third of the MRI scans recorded in clinical settings make use of contrast agents, mainly Gd(III) complexes (Caravan et al. 1999). The effectiveness of a Gd(III) complex to act as MRI contrast agent is first assessed by measuring its relaxivity, i.e., the relaxation enhancement of water protons observed for a millimolar solution of the contrast agent. In the past 15 years, a number of papers addressing the relationship between structure/dynamics and relaxivity of Gd(III) complexes have been published. This has led to a substantial advancement of our understanding of the structural, dynamic, and electronic parameters determining the relaxivity of paramagnetic chelates.

In addition to acting as a catalyst for the relaxation processes of tissutal water protons, a potential MRI-CA has to fulfill several requirements related to tolerance, safety, toxicity, stability, osmolality, viscosity, biodistribution, elimination, and metabolism. The currently used Gd(III) chelates are based on polyaminocarboxylate ligands (Scheme 1), either linear or macrocyclic molecules. All these ligands form very stable complexes (Table 1) so that the risk of dissociation is so low that the danger of acute toxic effects occurring after injection of gadolinium chelates is practically nonexistent with all the products currently in use.

The study of the central nervous system (CNS) is the primary clinical indication for the use of extracellular Gd(III) agents. The majority of these pathologies are brain tumors, and three quarters of them are represented by metastases occurring in patients undergoing treatment for systemic cancer (Fig. 1). Other brain diseases, such as multiple sclerosis and cerebral injuries can be also investigated by contrast-enhanced MRI.

There are several other indications for the use of CAs outside SNC. For instance, in the diagnosis of breast cancer, MRI with contrast agents is becoming an alternative diagnostic procedure to mammography. Particularly interesting is the dynamic use of contrast agents effect. The breast is imaged repeatedly over the first few min-



Scheme 1. Polyaminocarboxylate ligands, either linear or macrocyclic, of currently used Gd(III) chelates as commercial MRI contrast agents

utes following contrast agent administration, and a graph reporting the increase of signal for a selected region of interest is plotted as a function of time. The kinetics of the distribution of the contrast agents in the extravascular space is related to the vascular permeability. Neo-formed vessels functional to the tumor growth display a permeability much higher than normal capillaries and the corresponding

Table 1. Clinically accepted Gd(III)-based contrast agents

Complex	Brand name	Company	Log K_{GdL} (8)
Gd-DTPA	Magnevist	Schering	22.5
Gd-DOTA	Dotarem	Guerbet	24.7
Gd-HPDO3A	ProHance	Bracco	23.8
Gd-DO3A-butrol	Gadovist	Schering	20.8
Gd-DTPA-BMA	Omniscan	Nycomed-Amersham	16.8
Gd-DTPA-BMEA	OptiMARK	Mallinckrodt	16.8
Gd-BOPTA	MultiHance	Bracco	22.6
Gd-EOB-DTPA	Eovist	Schering	23.5

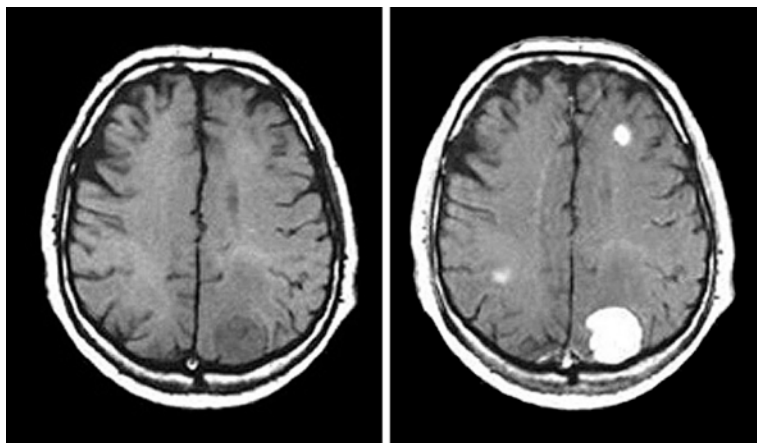


Fig. 1. Metastases in the brain of a patient with brain tumor. The metastases are detected upon intravenously administration of GdDTPA (*right*). Blood vessels (capillaries) are typically quite leaky to small molecules like GdDTPA, allowing them to enter the extracellular space. In the brain, however, the cells forming the walls of capillaries have very tight junctions and prevent small molecules leaving the intravascular space, thereby forming a blood-brain barrier (BBB). Tumors and other pathologies of CNS cause impairment of the BBB, thus allowing the contrast agent to leak from capillaries into extracellular fluid

areas are therefore characterized by high signal intensity (Padhani 2002). Of course, dynamic enhanced MRI is applied to demonstrate the aggressive nature of tumors in several other areas.

The new landscape of molecular imaging applications requires the development of a novel class of CAs characterized by higher contrasting ability and improved targeting capabilities. In this survey, we intend to tackle some basic issues that are of fundamental importance for the use of Gd(III)-based systems in molecular imaging applications, namely: (1) actual understanding of the determinants of T1-relaxivity of Gd(III) complexes, and how to proceed to attain very high relaxivities; (2) how one may envisage efficient routes for the delivery of a high number of Gd(III) complexes at the site of interest; and (3) the most practical ways to pursue the cell-internalization of a high number of Gd(III) complexes.

6.2 Determinants of Relaxivity

First of all, any MRI CA should be endowed with high thermodynamic and kinetic stability, and have at least one water molecule coordinated to the metal ion in fast exchange with the bulk water. This would allow strong influence over the relaxation process of all protons present in the solvent in which the CA is dissolved. The Gd(III) chelate efficiency is commonly estimated *in vitro* through the measure of its relaxivity (r_1); that for commercial CAs as Magnevist, Dotarem, Prohance, and Omniscan is around 3.4–3.5 mM⁻¹ s⁻¹ (at 20 MHz and 39°C). The observed longitudinal relaxation rate (R_1^{obs}) of the water protons in an aqueous solution containing the paramagnetic complex is the sum of three contributions (Banci et al. 1991): (a) the diamagnetic one, whose value corresponds to proton relaxation rate measured in the presence of a diamagnetic (La, Lu, Y) complex of the same ligand; (b) the paramagnetic one, relative to the exchange of water molecules from the inner coordination sphere of the metal ion with bulk water (R_{1p}^{is}); and (c) the paramagnetic one relative to the contribution of water molecules that diffuse in the external coordination sphere of the paramagnetic center (R_{1p}^{os}). Sometimes also a fourth paramagnetic contribution is taken in account, that is due to the presence of mobile protons or water molecules

(normally bound to the chelate through hydrogen bonds) in the second coordination sphere of the metal (Botta 2000). The inner sphere contribution is directly proportional to the molar concentration of the paramagnetic complex, to the number of water molecules coordinated to the paramagnetic center, q , and inversely proportional to the sum of the mean residence lifetime, τ_M , of the coordinated water protons and their relaxation time, T_{1M} . This latter parameter is directly correlated to the sixth power of the distance between the metal center and the coordinated water protons and depends on the molecular reorientational time, τ_R , of the chelate, on the electronic relaxation times, T_{iE} ($i=1, 2$), of the unpaired electrons of the metal (which depend on the applied magnetic field strength) and on the applied magnetic field strength itself (Fig. 2). The outer sphere contribution depends on T_{iE} , on the distance of maximum approach between the solvent and the paramagnetic solute, on the relative diffusion coefficients and again on the magnetic field strength (Aime et al. 1998). The dependence of R_{1p}^{is} and R_{1p}^{os} on magnetic field is very

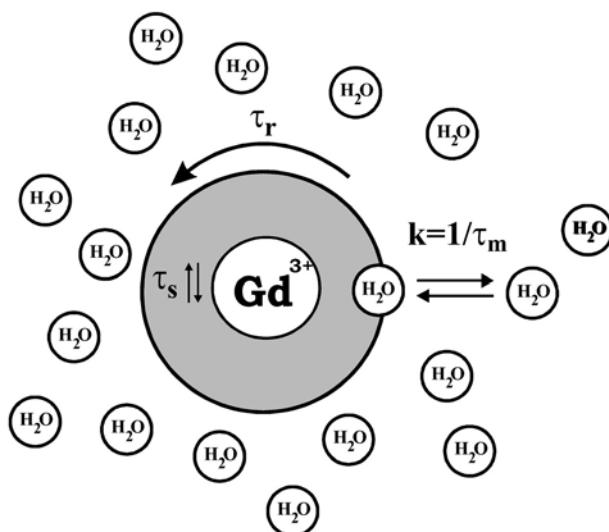


Fig. 2. Schematic representation of relaxation mechanism in an aqueous solution containing a Gd(III)-complex

important because from the analysis of the magnetic field dependence allows the determination of the principal parameters characterizing the relaxivity of a Gd(III) chelate. This information can be obtained through an NMR instrument in which the magnetic field is changed (Field-Cycling Relaxometer) to obtain the measure of r_1 on a wide range of frequencies (typically 0.01–50 MHz). At the frequencies most commonly used in commercial tomographs (20–63 MHz), r_1 is generally determined by the τ_R of the chelate so that high molecular weight systems display a higher relaxivity. A quantitative analysis of r_1 dependence on the different structural and dynamic parameters shows that, for systems with long τ_R (e.g., protein bound complex), the maximum attainable r_1 values can be achieved through the optimization of τ_M and T_{ic} (Banci et al. 1991).

6.3 How to Improve Relaxivity?

6.3.1 Interactions of Gd(III) Complexes with Proteins

Upon interacting with a macromolecule, the relaxation induced by Gd(III) chelates usually displays remarkable changes, primarily related to the increase of the molecular reorientational time τ_R on going from the free to the bound form, which results in a marked increase of the inner sphere R_1^{is} term. From the measurement of the relaxivity enhancement, it is possible to assess the affinity (and the number of binding sites) between the interacting partners (Dwek 1973). Quantitatively, in the presence of a reversible interaction between the paramagnetic species and the macromolecule, the observed enhancement depends on both the molar fraction of the macromolecular adduct χ^b and the relaxivity of the paramagnetic species bound to the macromolecule in the all-bound limit (r_1^b).

Human serum albumin (HSA) has been by far the most investigated protein for binding of Gd(III) chelates. Besides the attainment of high relaxivities, a high binding affinity to HSA enables the Gd(III) chelate with a long intravascular retention time, which is the property required for a good blood-pool agent for MR angiography. In blood, HSA has a concentration of about 0.6 mM and its main physiological role deals with the transport of a huge number of sub-

Table 2. Affinity constant and relaxivity of the adducts of some Gd(III) complexes with HSA, calculated at 0.47 T and 298 K. The coordinated water exchange lifetime of free complexes is also reported

Metal complex	$n \times K_A$ (M^{-1})	r_1^b ($mM^{-1}s^{-1}$)	τ_M (ns)	Reference
[Gd-DOTA(BOM)(H ₂ O)] ⁻	$< 1 \cdot 10^2$			Aime 1996 a
<i>Cis</i> -[Gd-DOTA(BOM) ₂ (H ₂ O)] ⁻	$6.4 \cdot 10^2$	35.2	175	Aime 1996 a
<i>Trans</i> -[Gd-DOTA(BOM) ₂ (H ₂ O)] ⁻	$7.2 \cdot 10^2$	44.2	130	Aime 1996 a
[Gd-DOTA(BOM) ₃ (H ₂ O)] ⁻	$3.4 \cdot 10^3$	53.2	80	Aime 1996 a
MS-325	$3.0 \cdot 10^4$	35.0	250	Aime 1999 c
[Gd-BOPTA (H ₂ O)] ²⁻	$4.0 \cdot 10^2$	33.0	280	Aime 2001; Aime 1999 b
[Gd-DTPA(BOM) ₂ (H ₂ O)] ²⁻	$3.6 \cdot 10^3$	28.2	260	Aime 2001; Aime 1999 b
[Gd-DTPA(BOM) ₃ (H ₂ O)] ²⁻	$4.0 \cdot 10^4$	44.0	180	Aime 1999 c
[Gd-DOTA-IOP(H ₂ O)] ⁻	$6.2 \cdot 10^2$	24.1	730	Aime 2001
[Gd-DOTA-IOP _{sp} (H ₂ O)] ⁻	$2.9 \cdot 10^3$	20.8	550	Aime 2001
[Gd-DOTA-TIB _{sp} (H ₂ O)] ⁻	$5.3 \cdot 10^2$	23.2	630	Aime 2001
[Gd-DTPA-IOP(H ₂ O)] ²⁻	$3.8 \cdot 10^2$	16.1	860	Aime 2001
[Gd-DTPA-IOP _{sp} (H ₂ O)] ²⁻	$4.8 \cdot 10^3$	19.9	630	Aime 2001

strates (Carter and Ho 1994). For many of them, the binding region has been identified on the basis of extensive competitive assays. Now, the availability of solid state X-ray crystal structure of HSA allows more insight into the structural details of the binding interaction. The information gained from the studies of the interaction of the various substrates to HSA has been very important in addressing the design of Gd(III)-based blood-pool agents.

In Table 2 a list of Gd(III) complexes and the relevant parameters of their binding interaction to HSA are reported.

Although the theory of the paramagnetic relaxation foresees relaxivities up to 100–120 $mM^{-1} s^{-1}$ (at 20 MHz) for complexes bound to macromolecular systems, the data listed in Table 1 show r_1^b values significantly lower than the predicted ones. The primary reason for the quenching of the relaxation enhancement is often associated to the occurrence of a long exchange lifetime, τ_M , of the coordinated water. This may be easily checked by measuring the relaxivity as a function of temperature. The detection of a higher r_1^b value as the

temperature is increased is an unambiguous indication of the occurrence of a too-long τ_M value.

6.3.2 Effect of the Water Exchange Rate on Relaxivity

Slow rates of the coordinated water appear to be primarily characteristic of the complex rather than a consequence of the binding to the protein. Thus, for the attainment of high relaxivities, one has to avoid Gd(III) chelates displaying slow exchange rates. The rationale which accounts for the water exchange rates in linear and cyclic polyaminocarboxylate Gd(III) complexes has been elucidated in a number of systems (Aime et al. 2001; Powell et al. 1996). In short, the water-exchange process for the enneacoordinate Gd(III) complexes follows an idealized dissociative pathway. This may be represented by a simple diagram involving the transition state where the metal ion has reduced its coordination number from 9 to 8 (Fig. 3).

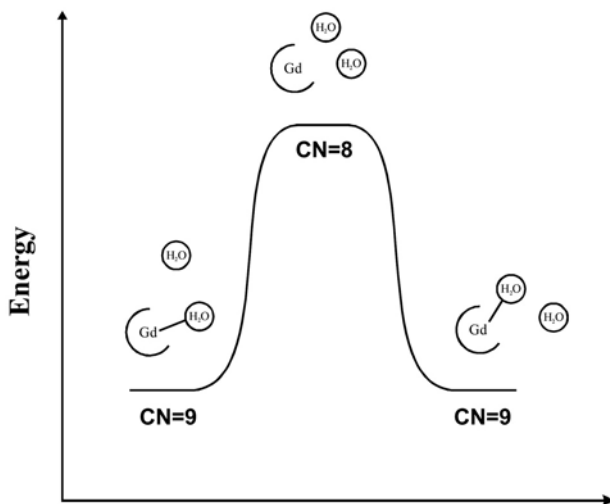


Fig. 3. Energy diagram for the idealized dissociative water exchange mechanism in enneacoordinate Gd(III) complexes

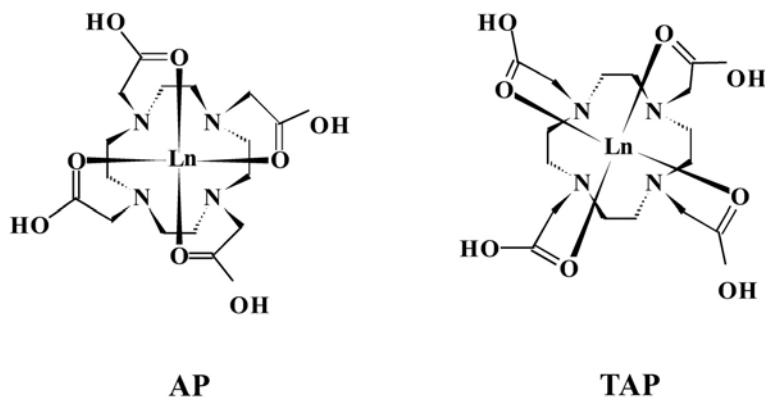


Fig. 4. Structure of the Square Antiprismatic (SA) and Twisted Square Antiprismatic (TSA) isomers in lanthanide DOTA-like complexes

It follows that fast exchange rates can be pursued by decreasing the activation energy and this goal can be addressed either by destabilizing the ground state or stabilizing the intermediate state. Moreover, it has been shown that for DOTA-like systems there is a subtle structural relationship between the exchange rate of the coordinated water and the actual isomeric form. In fact, this class of complexes exists in solution as a mixture of two structural isomers, namely the square antiprismatic (AP) and the twisted square antiprismatic (TAP) isomer (Fig. 4; Aime et al. 1992).

The polyhedron of the AP isomer corresponds closely to the regular square antiprismatic geometry, whereas a twisted square antiprismatic coordination cage with a smaller tilt angle between the two square planes is assigned to the TAP isomer. The latter isomer displays a water exchange rate that is approximately 50 times faster than the corresponding rate in the AP isomer (Aime et al. 1999 a).

Thus, given the above considerations, the functionalization of a ligand for protein targeting requires the choice of a Gd(III) chelate that displays a fast exchange rate of the coordinated water.

In order to get more insight into the problem of why the relaxivity values obtained up to now are significantly lower than those predicted by the theory of paramagnetic relaxation, we have recently

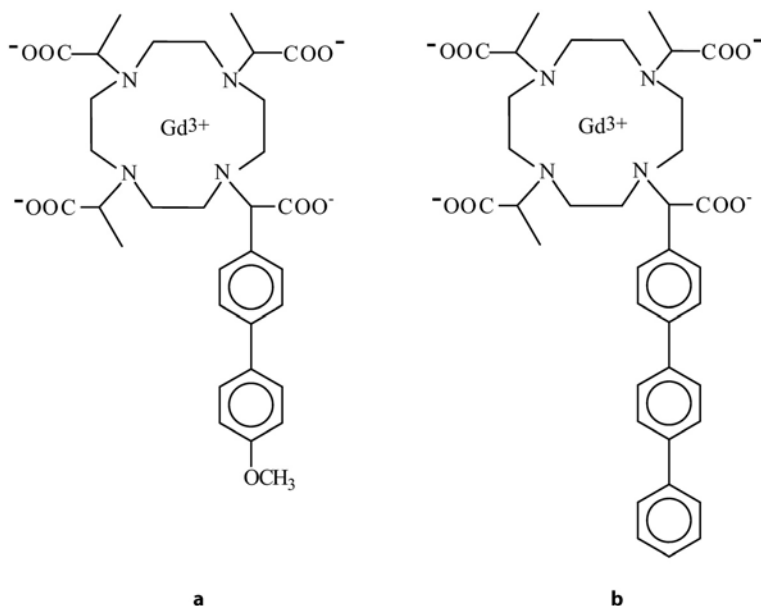


Fig. 5. Structure of two DOTMA derivatives

undertaken a detailed relaxometric study of the interaction of Gd-DOTMA derivatives with HSA (Aime et al., to be published). Gd-DOTMA displays a relatively fast exchange of the coordinated molecule, likely because it possesses a TAP-like structure as shown by $^1\text{H-NMR}$ spectra of the Eu(III) and Yb(III) analogs (Aime et al. 1996b; Di Bari et al. 2000). Two new ligands based on DOTMA structure have been synthesized (Fig. 5). $^1\text{H-NMR}$ spectra of Eu(III) complexes showed that the TAP geometry found for the parent DOTMA complexes is maintained. Complex A is soluble enough to allow the determination of the water exchange rate by $^{17}\text{O-T}_2$ measurements at variable temperature. The obtained value ($\tau_{\text{M}}^{298} = 65$ ns) indicates that the replacement of the methyl with the bulkier bis-Phenyl group does not affect the coordination cage, leaving unchanged the water exchange rate. The solubility of complex B was too low to pursue such measurement, but we may safely assume that its τ_{M}^{298} is similar to that determined for A.

Both A and B binds strongly to HSA, yielding K_a values of $2.7 \times 10^3 \text{ M}^{-1}$ and $9.5 \times 10^4 \text{ M}^{-1}$ respectively. r_1^b of the A/HSA adduct, at 298 K and 20 MHz, is equal to $35 \text{ mM}^{-1} \text{ s}^{-1}$. ^{17}O -measurements showed no difference between solutions containing the paramagnetic adduct and HSA alone. Clearly, the expected relaxation enhancement has been “quenched” by a direct interference of the donor groups on the surface of the protein with the inner hydration sphere of the Gd(III) ion. We could not determine whether it results in a replacement of the inner sphere water or simply in a dramatic elongation of its exchange lifetime. Thus, the bis-phenyl moiety does not appear long enough to protrude the chelate moiety outside the interference of the residues on the surface of the protein in proximity of the binding site. However, it is worthwhile to note that the observed relaxation enhancement is due to water molecules/mobile protons on the surface of the protein.

B contains a binding synthon made of three phenyl groups and resulted long enough to avoid such interference. Unfortunately, the low solubility of the adduct prevented the acquisition of ^{17}O -NMR VT spectra, but we got an indirect assessment of the occurrence of the fast exchange of the coordinated water by measuring the water proton relaxation rates as a function of temperature. As shown in Fig. 6, the observed relaxation rate displays an exponential decrease as the temperature increases, i.e., the typical behavior expected for systems not “quenched” by long exchange lifetimes of the coordinated water. However, the observed r_1^b for B/HSA adduct is only $43.5 \text{ mM}^{-1} \text{ s}^{-1}$, whereas the theory predicts much higher values (Fig. 6) for a system tumbling with the τ_R of HSA (30 ns) and the τ_M value of Gd-DOTMA.

We surmise that the limited relaxation enhancement has to be associated to a molecular reorientational correlation time, for the coordinated water, that is significantly shorter than that one of the macromolecule. This should not depend on an internal motion of the chelate as the binding through the tris-phenyl substituent is tight enough. Rather, the observed behavior should be related to an internal rotation of the coordinated water along its coordination axis, which overlaps with the overall motion of macromolecular adduct. If this suggestion is correct, a challenging question is posed to chemists: how to design a Gd-chelate whose coordinated water is in fast ex-

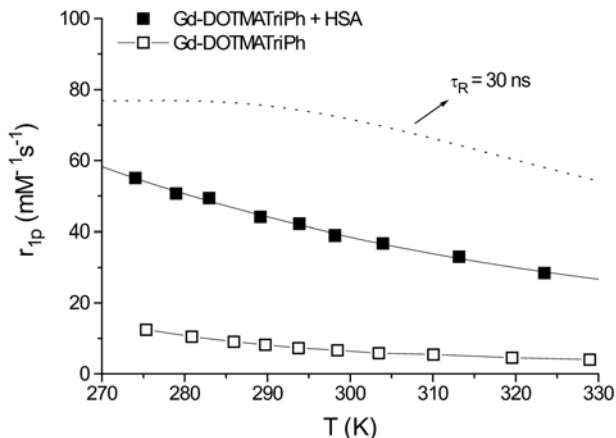


Fig. 6. Longitudinal proton relaxivity as a function of temperature of free complex B (*white boxes*) and of the adduct complex B/HSA (*black boxes*). The *dotted line* represents a simulation of the expected profile with $\tau_R=30$ ns and $\tau_M=65$ ns

change with the bulk (short τ_M) and “rigid” inside the coordination cage?

6.4 Targeting Cells with Gd(III) Chelates

Molecular imaging (Weissleder and Mahmood 2001) deals with *in vivo* characterization and measurement of biological processes at the cellular and molecular level. With molecular imaging, early diagnosis of disease will become possible as the detection of altered biochemical processes largely anticipates the anatomical changes that are at the basis of current diagnostic modalities.

Several modalities have contributed to the early stages of this innovative approach, namely PET, SPECT, MRI, and optical imaging. MRI-Gd(III)-based agents are much less sensitive than radionuclear and optical imaging probes. Therefore, molecular imaging based on MRI invariably involves the need of accumulating a high number of contrast-enhancing units at the site of interest. The basis for the design of a Gd-containing imaging probes is first dictated from the

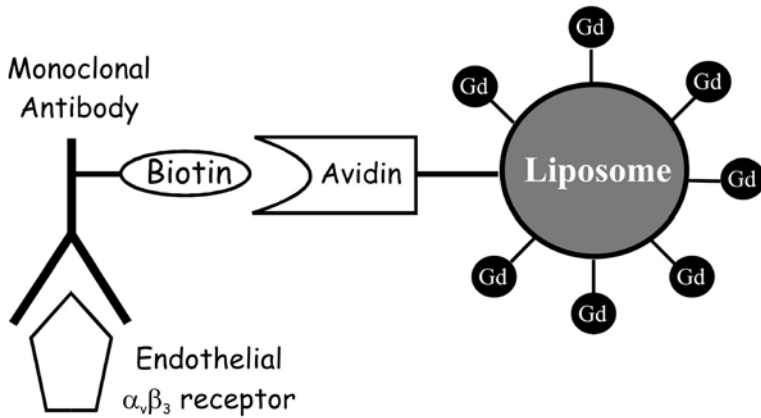


Fig. 7. Targeting of the endothelial integrin $\alpha_v\beta_3$ as a specific angiogenesis marker. The receptor is recognized by a biotinylated antibody that is then bound by an avidin moiety bearing a Gd(III)-loaded liposome

concentration and localization (vascular, extracellular matrix, on the cellular membrane, intracellular) of the target molecule (Aime et al. 2002a). Of course, the most accessible targets are those present on the surface of endothelial vessels. In principle, they can be visualized by a number of macromolecular conjugates containing many Gd(III) complexes endowed with the proper vector recognizing the given target. A nice example of targeting an endothelial site has been reported by Sipkins et al. (1998) in the targeting of a specific angiogenesis marker, the endothelial integrin $\alpha_v\beta_3$, whose presence has been shown to correlate with tumor grade. The imaging probe used in this work is a Gd-containing polymerized liposome. The target is first bound by a biotinylated antibody against $\alpha_v\beta_3$, which is successfully recognized by an avidin moiety on the surface of the liposome. Each liposome has a mean diameter of 300–350 nm, which appears suitable to avoid the uptake by the reticuloendothelial system (Fig. 7). This approach provided enhanced and detailed detection of rabbit carcinoma through the imaging of the angiogenic vasculature.

Recently, the same $\alpha_v\beta_3$ target has been addressed with lipidic nanoparticles containing a huge number of Gd-chelated units [94,400 Gd/

particle characterized by $r_1 = 19.1 \text{ s}^{-1} \text{ mM}^{-1}$ (per Gd), $r_1 = 1,800,000$ per particle]. One of the lipidic components is covalently bound to the $\alpha_v\beta_3$ -integrin peptidomimetic antagonist (Winter et al. 2003).

The large molecular size of these constructs limits their delivery to targets on the endothelial walls. To target receptors in solid tissues, other routes have to be followed. Bhujwala and coworkers (2003) have recently developed and applied a two-component Gd-based avidin-biotin system for the visualization of HER-2/scan receptors. The latter is a member of the epidermal growth factor family and it is amplified in multiple cancers. Their approach consisted of addressing the extracellular domain of the receptors by means of a biotinylated mAb. After clearance of the unbound mAb, Gd-labeled avidin is administered and binds, with high affinity, to the biotinylated mAb. The expression level of the receptor was estimated at 7×10^5 receptors/cell and the average number of Gd-DTPA units per avidin molecule was 12.5. The method has been successfully applied in an experimental mouse model of breast carcinoma.

An interesting route to MR signal amplification has been developed by Weissleder and coworkers (2002). Their approach is based on enzyme-mediated polymerization of paramagnetic substrates into oligomers of higher relaxivity. As substrates they used Gd-chelates functionalized with phenolic substituents which undergo rapid condensation in the presence of H_2O_2 and peroxidase. The increased molecular size of the oligomeric structures causes an increase of the molecular reorientational time which, in turn, results in an increase of the observed relaxivity. This approach has been applied to the imaging of E-selectin-peroxidase conjugate.

As far as the cell internalization of Gd-chelates is concerned, several routes have been explored:

1. Via Pinocytosis. Pinocytosis is the cell-internalized portion of the surrounding fluid by means of the invagination of its membrane and formation of small vesicles (≤ 150 nm diameter) called endosomes. Therefore, incubation of cells, for a sufficiently long time, in a medium containing the imaging probe at relatively high concentration leads to its internalization at amounts that may be sufficient for MRI visualization. Among a number of systems we have considered, the neutral, highly hydrophilic GdHPDO3A is a good candidate for la-

belonging stem cells by the pinocytotic route (Aime et al., in press). The *in vivo* MR visualization of labeled stem cells will allow their monitoring after transplantation. In a typical experiment of uptake via pinocytosis, a few million stem cells are incubated in a culture medium containing GdHPDO3A in mM concentration range (10–50 mM) for few hours. Upon incubation no saturation effect is observed and the amount of taken up Gd is linearly proportional to the concentration of the paramagnetic agent in the incubation medium. Once cell internalized, the GdHPDO3A molecules end up entrapped in endosomic vesicles as can be seen by observing the cells incubated with EuHPDO3A at the confocal microscope. In fact, Gd and Eu chelates with the same ligands display the same chemical/biological behavior, and the fluorescent response of EuHPDO3A acts as a histological reporter of the localization of GdHPDO3A in the cell. We have proved the potential of this approach by observing a mouse model of angiogenesis, on which blood-derived endothelial progenitor cells (EPCs) have been implanted subcutaneously, within a matrigel plug. After few days, the histologic examination showed large capillary structure transposing the gel plugs. MR images parallel histologic findings as hyperintense spots corresponding to the labeled cells were clearly detected. In Figure 8, we report a MR image taken 14 days after implantation. As control, matrigel-embedding unlabelled cells implanted in the same conditions are always negative for MRI signal.

The cell-labeling procedure described above appears to have general applicability. We have tested it on several tumor cell lines, obtaining invariantly a very efficient uptake with no apparent cytotoxicity. Likely, the entrapment of GdHPDO3A into the endosomic vesicles prevents any impact of the paramagnetic agent on relevant cellular process, meanwhile maintaining the full accessibility to cytoplasmatic water molecules.

2. Via Phagocytosis. Phagocytosis is the process of internalization of particles by cells endowed with phagocytic activity. In such a case, this route appears highly efficient for a single-step internalization of a large amount of imaging probes. However, to be effective on MR images, Gd-chelates must be water soluble. Therefore, the particles must be biodegradable in order to release soluble Gd chelates once

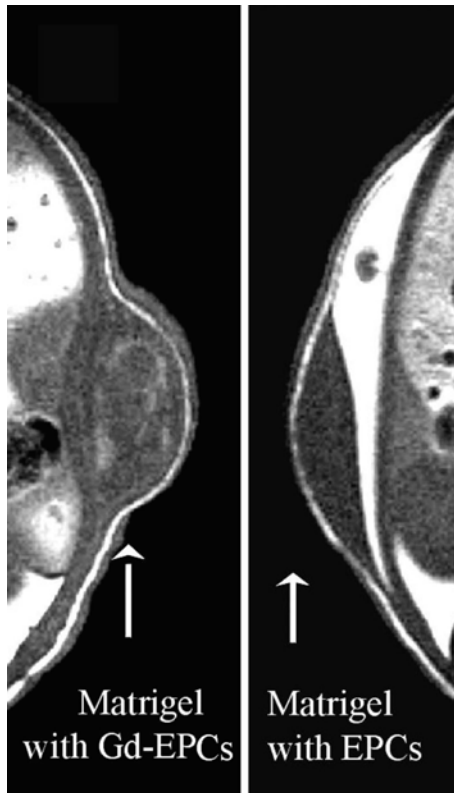


Fig. 8. In vivo T_1 -weighted spin echo MR image (7.05 T) of EPCs labeled with GdHPDO3A (*left*). The cells are dispersed into a subcutaneous matrigel plug 7 days after the implantation. On the *right* is the control image of the same in the absence of the paramagnetic label

internalized into phagocytic cells. One may envisage several ways for the release of the Gd chelates. For instance, one may think of gel nano-particles of chitosan loaded with negatively charged Gd-chelates. Such particles (200–400 nm diameter) are easily phagocytosed and slowly degraded once internalized into the cells (S. Aime et al., unpublished results). Another approach to biodegradable Gd-containing particles has been pursued by designing particles whose

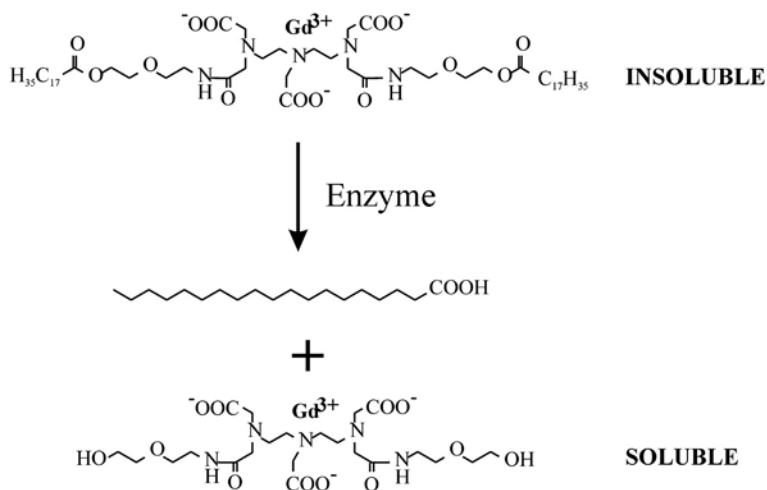


Fig. 9. The insoluble system is represented by a Gd-DTPA-like complex functionalized with a long aliphatic chain which is bound to the chelate moiety through an ester bond. The solubilization is obtained through the enzymatic cleavage of the ester bonds yielding to a soluble Gd(III) complex

insolubility is a property of the Gd-chelates themselves (Aime et al. 2002b). This goal is easily reached by introducing long aliphatic chains on the surface of the ligand. However, one can control the fate of these systems by means of the functionality used to link the insolubilizing moiety to the Gd-chelate. In fact, by using ester or peptidic functionalities, the insolubilizing synthon can be displaced from the Gd chelates by the activity of the proper enzyme (Fig. 9).

3. *Via Receptors.* Cell-internalization *via* receptors is the route of choice in a number of nuclear medicine assays. For MRI, the design of the imaging probe requires the attachment of one or more Gd(III)-chelates to the ligand molecule. Such structural modification may drastically affect the internalization process with respect to the mechanism occurring for the native ligand.

In order to deal with a system whose structural characteristics were unaltered by the loading with Gd(III) chelates, we choose Apoferritin because it allows the imaging probes to be entrapped inside

its inner cavity (Aime et al. 2002b). The exterior of such Gd(III)-loaded Apoferritin is exactly the same as in the parent Ferritin and then, once administered intravenously, it is quickly cleared-up by the proper receptors on hepatocytes (Osterloch et al. 1996). The process of loading Apoferritin with GdHPDO3A first entails the dissociation of the protein into subunits at pH 2 followed by its reforming at pH 7, thereby trapping the solution components (e.g., GdHPDO3A) within its interior. In such a system, water can freely diffuse through the channels formed at the intersection of the protein subunits (10 channels), but the larger GdHPDO3A molecules cannot. The relaxivity shown by each GdHPDO3A entrapped in the Apoferritin cavity is very high (approximately $80 \text{ s}^{-1} \text{ mM Gd}^{-1}$ at 20 MHz and 25°C). It has been possible to assess that the Gd-loaded Apoferritin maintains its integrity upon the cell internalization process as the relaxivity observed for the cytoplasmatic extract corresponds to that of the intact system. Finally, the amount of cell-internalized Gd-loaded Apoferritin is similar to that reported for the native Ferritin (6.5×10^6 molecules per cell in 6 h).

4. Via Receptor-Mediated Endocytosis. This is probably the most common route for the internalization of Gd(III) chelates as it is expected to occur any time a given ligand is modified by attaching one or more Gd-chelating units. Thus, the internalization process is no longer the one followed by the native ligand but the binding to the receptor stimulates an endocytotic process which starts with the inflection of a portion of cellular membrane and ends up with the welding of its extremities. Through this process, a number of substances remain entrapped in endosomic vesicles, primarily the molecules bound to the membrane or in close proximity of the portion of membrane involved in the endosome formation.

Weiner et al. (1997) showed that the uptake of a folate-conjugate dendrimer into tumor cells overexpressing high affinity folate receptor (hFR) occurs through this type of endocytotic pathway.

Another example of receptor-mediated endocytosis of a large dendrimer has been recently reported (Kobayashi and Brechbiel 2003). The macromolecular construct comprised of Avidin and a biotinylated dendrimer bearing 254 GdDTPA chelates (AV-G6Gd) has shown to accumulate *in vitro* into SHIN3 cells (a cell line obtained

originally from human ovarian cancer) 50-fold greater than GdDTPA. The internalization process is driven by avidin molecule, a glycoprotein that binds to β -D-galactose receptors which are present on these tumor cells.

Although not yet proven, it is likely that receptor-mediated endocytosis occurs with a number of systems in which the imaging Gd-probes are linked either to peptides as targeting vectors that bind to specific receptors or to nutrient or pseudo-nutrient moieties that interact with the proper transporter upregulated in tumor cells.

5. Via Transmembrane Carrier Peptides. Another route to enter cells with Gd(III) chelates is based on the use of membrane translocation peptides which have been proven useful for the internalization of a number of substrates like proteins, oligonucleotides, and plasmid DNA. For instance, Bhorade et al. (2000) showed that GdDTPA bound to 13-merHIV-tat peptide is efficiently internalized.

Another example has been recently reported by Allen and Meade (2003), who showed that GdDTPA conjugated to polyarginine (8–16 monomer units) is able to permeate all membranes.

Finally, along this line, an interesting development has been recently reported by Heckl et al. (2003). They synthesized an imaging probe consisting of a Gd-complex, a PNA (Peptide Nucleic Acid) sequence, and a transmembrane carrier peptide. Although the system enters any type of cell, it accumulates only in tumor cells because of the specific binding of the PNA moiety for the *c-myc* mRNA whose production is upregulated in those cells.

6.5 Concluding Remarks

Gd(III) chelates have played an important role in the development of clinical applications of MRI technique by adding relevant physiological information to the superb anatomical resolution attainable with this imaging modality.

More is still expected with the currently available contrast agents, especially in the field of dynamic contrast enhancement protocols reporting on changes of the vascular permeability associated with the staging and therapeutic follow-up of important pathologies. How-

ever, the major challenges are in the emerging field of molecular imaging where the competition with other imaging modalities can be very tight. Targeting of thrombi and atherosclerotic plaques by peptides functionalized with Gd(III) chelates appears to be the next goal for industrial research. The possibility of identifying and characterizing vulnerable plaques will certainly represent an important task. Clearly, there is a need for new ideas for enhancing the attainable relaxivity at higher fields as the 3-T indication for clinical imagers seems to be quite established. Moreover, it will be necessary to improve the efficiency of the available delivery systems and, possibly, to exploit suitable amplification procedures in order to reach the sensitivity required for the visualization of target molecules present at low concentrations.

The results herein surveyed show that there are several routes for cell entrapment of paramagnetic Gd-agents at concentrations sufficient for MRI visualization. The huge work carried out in a number of laboratories in the last two decades for the development of Gd-based MRI contrast agents provides an excellent platform for designing a new generation of probes for molecular imaging applications. Though one should not underestimate the difficulties that will arise when going from *in vitro* experiments to *in vivo* animal studies, we think that the available results suggest that Gd-chelates will have an important role in the armory of imaging probes for cellular and molecular imaging applications.

References

- Aime S, Botta M, Ermondi G (1992) Nmr-study of solution structures and dynamics of lanthanide(III) complexes of dota. *Inorg Chem* 31:4291–4299
- Aime S, Botta M, Fasano M, Geninatti Crich S, Terreno E (1996a) Gd(III) complexes as contrast agents for magnetic resonance imaging: a proton relaxation enhancement study of the interaction with human serum albumin. *J Biol Inorg Chem* 1:312–319
- Aime S, Botta M, Fasano M, Terreno E, Kinchesh P, Calabi L, Palestini L (1996b) A new ytterbium chelate as contrast agent in chemical shift imaging and temperature sensitive probe for MR spectroscopy. *Magn Res Med* 35:648–651
- Aime S, Botta M, Fasano M, Terreno E (1998) Lanthanide(III) chelates for NMR biomedical applications. *Chem Soc Rev* 27:19–29

- Aime S, Barge A, Bruce J, Botta M, Howard JAK, Moloney JM, Parker D, de Sousa AS, Woods M (1999 a) NMR, relaxometric, and structural studies of the hydration and exchange dynamics of cationic lanthanide complexes of macrocyclic tetraamide ligands. *J Am Chem Soc* 121:5762–5771
- Aime S, Botta M, Fasano M, Terreno E (1999b) Prototropic and water-exchange processes in aqueous solutions of Gd(III) chelates. *Acc Chem Res* 32:941–949
- Aime S, Chiaussa M, Digilio G, Gianolio E, Terreno E (1999c) Contrast agents for magnetic resonance angiographic applications: H-1 and O-17 NMR relaxometric investigations on two gadolinium(III) DTPA-like chelates endowed with high binding affinity to human serum albumin. *J Biol Inorg Chem* 4:766–774
- Aime S, Fasano M, Terreno E, Botta M (2001) In: Merbach AE, Tóth E (eds) *The chemistry of contrast agents in medical magnetic resonance imaging*. Wiley, Chichester, pp 193–241
- Aime S, Cabella C, Colombatto S, Crich SG, Gianolio E, Maggioni F (2002 a) Insights into the use of paramagnetic Gd(III) complexes in MR-molecular imaging investigations. *J Magn Reson Imaging* 16:394–406
- Aime S, Frullano L, Geninatti Crich S (2002b) Compartmentalization of a gadolinium complex in the apoferritin cavity: A route to obtain high relaxivity contrast agents for magnetic resonance imaging. *Angew Chemie Int Ed* 41:1017–1019
- Allen MJ, Meade TJ (2003) Synthesis and visualization of a membrane-permeable MRI contrast agent. *J Biol Inorg Chem* 8:746–750
- Banci L, Bertini I, Luchinat C (1991) Nuclear and electronic relaxation. VCH, Weinheim, pp 91–122
- Bhorade R, Weissleder R, Nakakoshi T, Moore A, Tung CH (2000) Macrocyclic chelators with paramagnetic cations are internalized into mammalian cells via a HIV-tat derived membrane translocation peptide. *Bioconjugate Chem* 11:301–305
- Bhujwala ZM, Artemov D, Mori N, Ravi R (2003) Magnetic resonance molecular imaging of the HER-2/neu receptor. *Cancer Res* 63:2723–2727
- Botta M (2000) Second coordination sphere water molecules and relaxivity of gadolinium(III) complexes: implications for MRI contrast agents. *Eur J Inorg Chem* 3:399–407
- Caravan P, Ellison JJ, McMurry TJ, Lauffer RB (1999) Gadolinium(III) chelates as MRI contrast agents: structure, dynamics, and applications. *Chem Rev* 99:2293–2352
- Carter D, Ho JX (1994) Structure of serum-albumin. *Adv Prot Chem* 45: 153–203
- Di Bari L, Pintacuda G, Salvadori P (2000) Solution equilibria in YbDOTMA, a chiral analogue of one of the most successful contrast agents for MRI, GdDOTA. *Eur J Inorg Chem* 75–82
- Dwek RA (1973) Nuclear magnetic resonance in biochemistry, applications to enzyme systems, Clarendon Press, Oxford, pp 174–283

- Heckl S, Pipkorn R, Waldeck W, Spring H, Jenne J, von der Lieth CW, Corban-Wilhelm H, Debus J, Braun K (2003) Intracellular visualization of prostate cancer using magnetic resonance imaging. *Cancer Res* 63:4766–4772
- Kobayashi H, Brechbiel MW (2003) Dendrimer-based macromolecular MRI contrast agents: characteristics and application. *Mol Imaging* 2:1–10
- Merbach AE, Tóth E (2001) The chemistry of contrast agents in medical magnetic resonance imaging. Wiley, Chichester
- Osterloh K, Aisen P (1989) Pathways in the binding and uptake of ferritin by hepatocytes. *Biochem Biophys Acta* 1011:40–45
- Padhani AR (2002) Dynamic contrast-enhanced MRI in clinical oncology: current status and future directions. *J Magn Res* 16:407–422
- Powell DH, Ni Dhubghaill OM, Pubanz D, Helm L, Lebedev HS, Schlaepfer W, Merbach AE (1996) Structural and dynamic parameters obtained from O-17 NMR, EPR, and NMRD studies of monomeric and dimeric Gd³⁺ complexes of interest in magnetic resonance imaging: an integrated and theoretically self consistent approach. *J Am Chem Soc* 118:9333–9346
- Rinck PA (2003) Magnetic resonance in medicine. ABW Wissenschaftsverlag, Berlin
- Sipkins DA, Cheresch DA, Kazemi MR, Nevin LM, Bednarski MD, Li KCP (1998) Detection of tumor angiogenesis in vivo by alpha(v)beta(3)-targeted magnetic resonance imaging. *Nat Med* 4:623–626
- Weissleder R, Mahmood U (2001) Molecular imaging. *Radiology* 219:316–333
- Weissleder R, Bogdanov A, Matuszewski L, Bremer C, Petrovski A (2002) Oligomerization of paramagnetic substrates result in signal amplification and can be used for MR imaging of molecular targets. *Mol Imag* 1:16–23
- Wiener EC, Konda S, Shadron A, Brechbiel M, Gansow O (1997) Targeting dendrimer-chelates to tumors and tumor cells expressing the high-affinity folate receptor. *Invest Radiol* 32:748–754
- Winter PM, Caruthers SD, Kassner A, Harris TD, Chinen LK, Allen JS, Lacy EK, Zhang HY, Robertson JD, Wickline SA, Lanza GM (2003) Molecular imaging of angiogenesis in nascent vx-2 rabbit tumors using a novel alpha(v)beta(3)-targeted nanoparticle and 1.5 tesla magnetic resonance imaging. *Cancer Res* 63:5838–5843
- Young IR (2000) Methods in biomedical magnetic resonance imaging and spectroscopy. Wiley, Chichester